YGHP-16-05

Stabilizing semilocal strings by polarization

Minoru Eto[1], Muneto Nitta[2] and Kohei Sakurai[1]

[1] *Department of Physics, Yamagata University, Yamagata, 990-8560, Japan*

[2] *Department of Physics, and Research and Education Center for Natural Sciences, Keio University, Hiyoshi 4-1-1, Yokohama, Kanagawa 223-8521, Japan*

arXiv:1608.03516v1 [hep-th] 11 Aug 2016

Abstract

Semilocal strings are vortices in the extended Abelian-Higgs model with two complex Higgs scalar fields among which a global $SU(2)$ symmetry acts. They are known to be stable (unstable against expansion) in type-I (II) superconductors, in which gauge field is heavier (lighter) than the Higgs scalar field. In this paper, we find that vortices can be stabilized in the whole parameter region including the type-II region by adding a potential term breaking the $SU(2)$ symmetry. We construct numerical solutions in various parameters and determine the vortex phase diagram consisting of six phases. In two phases, a vortex is polarized, that is, split into two half-quantized vortices with a certain distance, to form a vortex molecule, while in the rests a vortex is identical to the conventional Abrikosov-Nielsen-Olesen vortex.

1 Introduction

Magnetic fields are confined in the form of vortices or flux tubes in superconductors, macroscopically described by the Abelian-Higgs model, that is, a $U(1)$ gauge theory coupled with one complex Higgs scalar field [1, 2]. Vortices are called Abrikosov-Nielsen-Olesen (ANO) vortices or local vortices. Depending on the masses m_e and m_H of gauge and Higgs fields, respectively, the superconductor can be classified into type-I ($m_H < m_e$) or II ($m_e < m_H$). At the critical coupling ($m_e = m_H$), it is called Bogomol'nyi-Prasado-Sommerfield (BPS). For type-I, II and BPS superconductors, there exist attractive, repulsive, and no forces, respectively, between vortices. Superconductors are stable against applied magnetic fields when they are of type-II, constituting a vortex lattice inside it stabilized by repulsion among vortices. Vortices are cosmic strings in cosmology, and so relativistic dynamics have been studied well.

Semilocal cosmic strings are vortex strings in the extended Abelian-Higgs model with two Higgs complex scalar fields with an $SU(2)$ symmetry [3, 4]. Cosmological consequences of semilocal strings such as their effects on cosmic microwave background were studied in Ref. [5]. Semilocal cosmic strings reduce to $O(3)$ sigma model ($\mathbb{C}P^1$ model) lumps in strong gauge coupling limit [6], which are supported by the second homotopy group $\pi_2(M)$ and have size and phase moduli. The stability of semilocal strings were studied very well [6, 7]. As lumps, semilocal strings at critical coupling (BPS limit) have size and phase moduli and are marginally stable. At near critical coupling a potential is induced for the size modulus. In the type-II region in which the gauge boson is lighter than the Higgs boson, semilocal strings are unstable to expand, while they shrink to the ANO vortices and are stable in the type-I region in which the Higgs boson is lighter than the gauge boson. Non-Abelian semilocal cosmic strings have been studied recently [8, 9], which reduce to Grassmann sigma model lumps in strong gauge coupling limit. Reconnection of two colliding non-Abelin semilocal strings were also studied [10]. Other than semilocal strings, possible semilocal solitons were classified [11, 12], including codimension-four sigma model instantons [13, 14].

On the other hand, the topological charges of topological solitons supported by certain homotopy groups are usually quantized to be integers. However in certain situations, the minimum topological charge can be fractional. Typical examples are fractional magnetic vortices (flux tubes) in multi-component or multi-band superconductors [15, 16, 17, 18, 19, 20, 21] and fractional superfluid vortices in two-component [22, 23, 24, 25, 26, 27, 28, 29, 30], three-componet [31, 32], and multi-component [33, 34] Bose-Einstein condensates (BECs). For the system of N components, topological charge is fractionalized to be $1/N$ if VEVs are all equal. Each fractional vortex is a half-local and half-global vortex in superconductors while

it is a global vortex in BECs. $O(3)$ sigma model ($\mathbb{C}P^1$ model) lumps in 2+1 dimensions (or instanton in 2+0 dimensions) are characterized by $\pi_2(M)$. A lump can be decomposed into a vortex anti-vortex pair with fractional lump charges in the presence of a certain potential term [35, 36, 37, 38]. Topologically the same thing occurs for baby Skyrmions characterized by $\pi_2(M)$. One baby Skyrmion is decomposed into a vortex anti-vortex pair with fractional lump charges in the presence of the same type of the potential term [39, 40, 30]. As a 3+1 dimensional example, a Skyrmion characterized by the third homotopy group $\pi_3(M)$ can be decomposed into a monopole and anti-monopole pair with fractional Skyrmion charges in the presence of a certain potential term [41].

In this paper, we decompose a semilocal string into two half-quantized strings by introducing a potential term breaking the $SU(2)$ symmetry and show that semilocal strings become stable against expansion in the whole parameter region including type-II superconductors. Each fractional string has opposite charges $\pm 1/2$ of a global $U(1)$ symmetry of a subgroup of $SU(2)$, which is unbroken by the additional potential. We obtain numerical solutions for the fractional strings, and also investigate the asymptotic behaviors quite different from either the well-known ANO strings or usual semilocal strings. We find that the asymptotic behaviors of the profile function decay exponentially with the smallest masses of the fields at the bulk. We study the dependence of the polarization of the single semilocal string in all parameter region with the masses m_e, m_λ and m_η in detail. We find that the semilocal string is stable in the whole parameter region. Especially, the type II region $m_e < m_\lambda$ is divided into two phases. In one region, the unpolarized semilocal string, namely the type-II ANO solution, appears for $m_e < m_\lambda < m_e + m_\eta$. In the other region $m_\lambda > m_e + m_\eta$, the two Higgs fields have zeros at different points, namely the string is polarized. The displacement $|d|$ of the two zeros is larger for smaller m_e. It also increases as m_λ increase but saturates at a certain upper value.

The behaviors of asymptotics of the profile functions, that they exponentially decay with the smallest mass in the bulk, are similar [42, 43] to those of the semisuperfulid non-Abelian strings [44, 45] in the dense QCD, even though the roles of local and global symmetry are opposite to the model studied in this paper (namely, the Abelian symmetry is global and the non-Abelian symmetry is local). Thus, we believe that the phenomena that the smallest mass controls asymptotic behavior is common to strings in a wide range of physical model.

This paper is organized as follows. In Sec. 2, we review semilocal vortices in the $SU(2)$ symmetric model. In Sec. 3, we work out the vortex structure in the model with a broken $SU(2)$ symmetry. We construct numerical solutions with various parameters and determine the phase diagram. Section 4 is devoted to a summary and discussion. The numerical method that we use in this paper is explained in Appendix A.

2 The semilocal strings in an $SU(2)$ symmetric model

We consider the Abelian-Higgs model with a Higgs doublet $H = (H_1, H_2)$. The Lagrangian is given by

$$\mathcal{L} = -\frac{1}{4e^2}F_{\mu\nu}F^{\mu\nu} + \mathcal{D}_\mu H(\mathcal{D}^\mu H)^\dagger - V_0, \quad V_0 = \frac{\lambda^2}{2}\left(HH^\dagger - v^2\right)^2, \tag{2.1}$$

with $F_{\mu\nu} = \partial_\mu A_\nu - \partial_\nu A_\mu$ and $\mathcal{D}_\mu H = (\partial_\mu + iA_\mu)H$. The Lagrangian has a global $SU(2)$ symmetry under which the Higgs fields is transformed as the fundamental representation. In the vacua, both the gauge and flavor symmetry are spontaneously broken. The vacuum states are degenerate and form a vacuum manifold S^3 defined by

$$HH^\dagger = v^2. \tag{2.2}$$

By identifying each $U(1)$ gauge orbit as a point, the vacuum moduli is given by

$$\mathcal{M}_0 = \frac{SU(2)}{U(1)} \simeq \mathbb{C}P^1. \tag{2.3}$$

Therefore, the number of the physical Nambu-Goldstone modes is $\dim_{\mathbb{R}} \mathcal{M}_0 = 2$, and there is a massive Higgs mode with mass

$$m_\lambda = \sqrt{2}\lambda v. \tag{2.4}$$

At the same time, the photon gets mass

$$m_e = \sqrt{2}ev. \tag{2.5}$$

It is well-known that the model (2.1) admits solitonic strings, the so-called semilocal strings, even though the vacuum manifold is homotopically trivial $\pi_1(S^3) = 1$. It is a static solution of the classical equation of motion

$$\mathcal{D}_\mu\mathcal{D}^\mu H_a = \left[\lambda^2(v^2 - HH^\dagger)\right]H_a, \quad (a = 1, 2), \tag{2.6}$$

$$\frac{1}{e^2}\partial_\mu F^{\mu\nu} = -i\left(H\mathcal{D}^\nu H^\dagger - \mathcal{D}^\nu H H^\dagger\right). \tag{2.7}$$

It has been known that the semilocal string is dynamically stable only when the masses satisfy the relation for type-I superconductors

$$m_\lambda \leq m_e. \tag{2.8}$$

At the critical coupling $e = \lambda$ ($m_\lambda = m_e$), the equations of motion reduce to a set of the first order differential equations, so-called Bogomol'nyi equation,

$$(\mathcal{D}_1 + i\mathcal{D}_2)H = 0, \qquad \frac{1}{e^2}F_{12} = HH^\dagger - v^2. \tag{2.9}$$

Introducing the complex coordinate $z = x^1 + ix^2$ and $\partial_z = (\partial_1 - i\partial_2)/2$, the first equation can be solved by [46, 47]

$$H = ve^{-\frac{\psi(z,\bar{z})}{2}} H_0(z), \quad A_1 + iA_2 = -2i\partial_{\bar{z}}\psi, \tag{2.10}$$

where $H_0(z)$ is a 2-vector whose components are holomorphic functions of z and ψ is a complex scalar function of z and $\bar{z}$ determined below. In the following, we will set ψ to be real positive by fixing the $U(1)$ gauge degree of freedom. Plugging these into the second Bogomol'nyi equation, we end up with the master equation for the semilocal vortex

$$\frac{1}{2e^2v^2}\partial_i^2\psi = 1 - H_0 H_0^\dagger e^{-\psi}, \tag{2.11}$$

with $\partial_i^2 = \partial_1^2 + \partial_2^2$ and $F_{12} = -\frac{1}{2}\partial_i^2\psi$, and the boundary condition

$$\psi \to \log H_0 H_0^\dagger \quad \text{as} \quad |z| \to \infty. \tag{2.12}$$

The master equation determines ψ according to a given $H_0(z)$. H_0 is a pair of two polynomials $P_1(z)$ and $P_2(z)$ as

$$H_0(z) = (P_1(z),\ P_2(z))\,. \tag{2.13}$$

The tension (mass per unit length) of the semilocal strings at the critical coupling is determined only by the quantized magnetic flux $2\pi k$ with an integer k as

$$T = 2\pi v^2 |k|. \tag{2.14}$$

The integer k is related to the highest degree of the polynomials in $H_0(z)$. Indeed, ψ asymptotically behaves as $\psi \to \log|z|^{2k} + \cdots$, then we find

$$-\frac{1}{2\pi}\int dx^1 dx^2\ F_{12} = \frac{1}{4\pi}\int dx^1 dx^2\ \partial_i^2\psi = \frac{1}{4\pi}\oint_{S^1_\infty} dS\ \vec{n}\cdot\vec{\nabla}\psi = k. \tag{2.15}$$

The minimal BPS semilocal string is characterized by the following H_0 with 2 complex parameters

$$H_0 = (z - z_1,\ z - z_2)\,, \quad \{z_a\} \in \mathbb{C}^2, \tag{2.16}$$

where we have chosen the *symmetric* boundary configuration $H \to (v,\ v)/\sqrt{2}$ up to the overall $U(1)$ phase. Since H is proportional to H_0, the a-th Higgs field becomes zero at $z = z_a$, and so one might expect 2 peaks in energy density for $k = 1$ configuration, but it is not the case. What we observe is only a single peak. Namely, the energy distribution is always axially symmetric, and no substructures can be found.

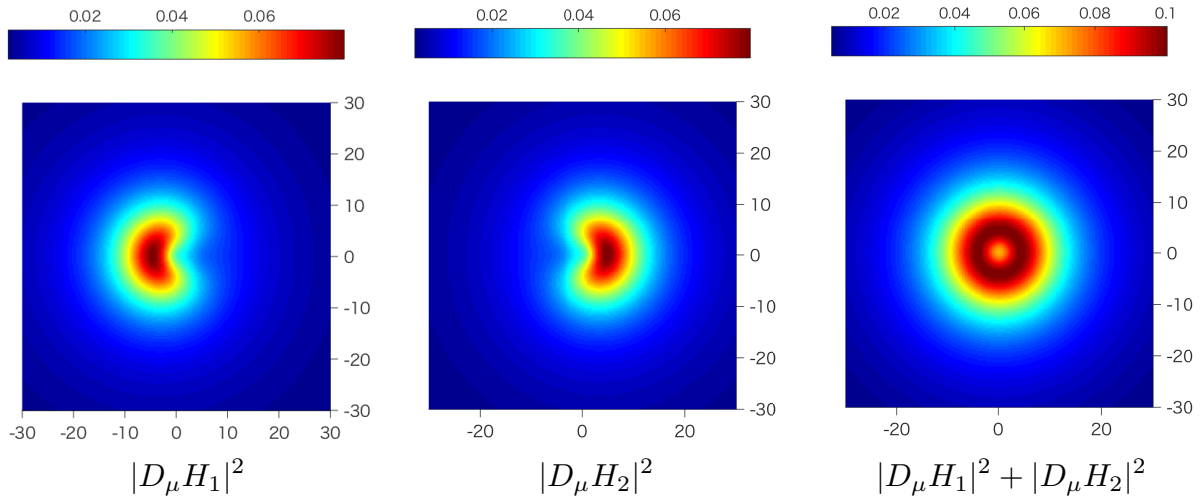

Figure 1: The scalar kinetic energies for the single BPS semilocal string with $H_0 = (z-5,\ z+5)$ in $N_{\rm F} = 2$ case.

As an example, we show the kinetic energy densities $|\mathcal{D}_\mu H_1|^2$, $|\mathcal{D}_\mu H_2|^2$ and $|\mathcal{D}_\mu H_1|^2 + |\mathcal{D}_\mu H_2|^2$ for $H_0 = (z-5,\ z+5)$ in Fig. 1. Nevertheless the individual kinetic energies have peaks at apparently different points, the sum $|\mathcal{D}_\mu H_1|^2 + |\mathcal{D}_\mu H_2|^2$ is axially symmetric and has only one peak at the origin. The gauge kinetic term and scalar potential term are also axially symmetric, so no inner structures appear. This may easily be understood by looking at another solution which is just obtained by rotating H_0 given in Eq. (2.16) with a certain $SU(2)$ flavor transformation to the following one

$$H_0 = (z - z_1,\ z - z_2) \quad \to \quad \sqrt{2}\left(z - \frac{z_1+z_2}{2},\ \frac{z_1 - z_2}{2}\right). \tag{2.17}$$

It is now clear that only the first Higgs field vanishes at the center of mass $z = \frac{z_1+z_2}{2}$ while the second component never touches zero. Thus, it is quite natural to regard $(z_1 + z_2)/2$ as the position of the semilocal string, indeed the energy density has a single peak there. The parameter $(z_1 - z_2)/2$ in the second component of H_0 can be decomposed into the phase modulus and the "distance" $|z_1 - z_2|$ which represents the thickness (size) of the semilocal string. When $|z_1 - z_2|$ is zero, the second component in the Higgs field plays no role, namely is everywhere zero, so that the semilocal string becomes the ANO string in the Abelian-Higgs model with a single complex field. The semilocal string for $|z_1 - z_2| > 0$ is a fatter string. In the opposite limit $|z_1 - z_2| \to \infty$, the first component is negligible compared to the second one. This means that the semilocal string gets fat and dilutes as $|z_1 - z_2|$ being increased, and finally disappears with the vacuum left behind.

Once we leave from the critical coupling $m_e = m_\lambda$, the semilocal string is no longer BPS. As a consequence, all the moduli fields except for the center of mass are gone. Accordingly, the moduli $z_1 - z_2$ of the BPS semilocal string is lifted by an effective potential. A schematic image of the effective potential is shown in Fig. 2. It falls down to zero for $m_\lambda < m_e$ (type I) or runs away to infinity for $m_e < m_\lambda$ (type II). In other words, the semilocal string in $m_\lambda < m_e$ is the same as the ANO string of the type I, while one in $m_e < m_\lambda$ is unstable to dilute.

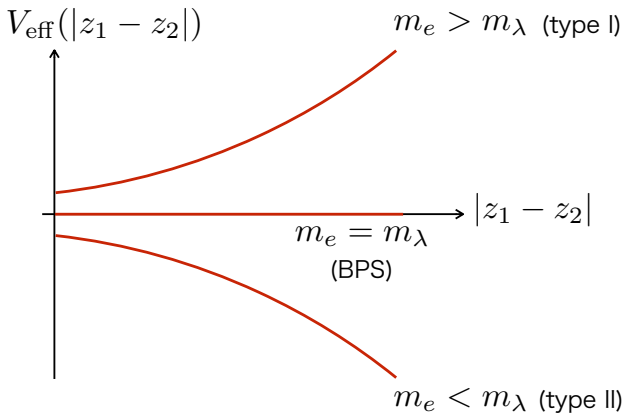

Figure 2: A schematic image for an effective potential of the size moduli $|z_1 - z_2|$.

3 Polarization of semilocal strings

3.1 The $SU(2)$ breaking interaction

In this section, we will introduce polarization for the semilocal string. As we will explain below, the polarization cannot be manifestly defined for the semilocal strings in the $SU(2)$ symmetric model reviewed in the previous section. It will turn out that a key ingredient for the polarization is breaking of $SU(2)$ symmetry. For that purpose, we will include an additional Higgs potential to the Lagrangian $\mathcal{L}$ given in Eq. (2.1),

$$V_1 = \frac{\eta^2}{2}(H\tau_3 H^\dagger)^2 = \frac{\eta^2}{2}(|H_1|^2 - |H_2|^2)^2, \tag{3.1}$$

with τ_3 being the third element of Pauli matrix. The flavor symmetry $SU(2)$ is explicitly broken to the $U(1)$ subgroup generated by τ_3.[1]

[1] Note that the additional Higgs potential (3.1) is identical to the D-term potential in the context of the supersymmetric extension of our model when we gauge the $U(1)$ symmetry generated by τ_3.

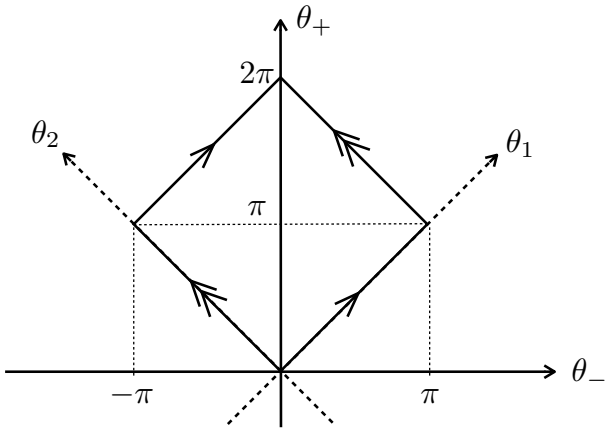

Figure 3: Vacuum manifold

The additional potential reduces the original vacuum manifold S^3 ($|H_1|^2 + |H_2|^2 = v^2$) to $S^1 \times S^1$ defined by the following condition

$$|H_1|^2 = |H_2|^2 = \frac{v^2}{2}. \tag{3.2}$$

The vacuum manifold is parametrized by the phases of H_1 and H_2 as

$$H_1 = \frac{v}{\sqrt{2}} e^{i\theta_1} = \frac{v}{\sqrt{2}} e^{i\theta_+ + i\theta_-}, \quad H_2 = \frac{v}{\sqrt{2}} e^{i\theta_2} = \frac{v}{\sqrt{2}} e^{i\theta_+ - i\theta_-}. \tag{3.3}$$

The gauge orbit is parametrized by θ_+ while the global orbit is parametrized by θ_-. The vacuum manifold is illustrated in Fig. 3.

To see the mass spectra, let us consider small fluctuations around the vacuum $H_1 = \frac{v}{\sqrt{2}} + f_1 + ig_1$ and $H_2 = \frac{v}{\sqrt{2}} + f_2 + ig_2$. The quadratic Lagrangian is given by

$$\begin{aligned} \mathcal{L}^{(2)} &= -\frac{1}{4e^2}\tilde{F}_{\mu\nu}^2 + \left(\partial_\mu \frac{f_1+f_2}{\sqrt{2}}\right)^2 + \left(\partial_\mu \frac{f_1-f_2}{\sqrt{2}}\right)^2 + \left(\partial_\mu \frac{g_1-g_2}{\sqrt{2}}\right)^2 \\ &\quad + v^2\tilde{A}_\mu^2 - 2\lambda^2 v^2 \left(\frac{f_1+f_2}{\sqrt{2}}\right)^2 - 2\eta^2 v^2 \left(\frac{f_1-f_2}{\sqrt{2}}\right)^2, \end{aligned} \tag{3.4}$$

where we have defined $\tilde{A}_\mu = A_\mu + v^{-1}\partial_\mu \frac{g_1+g_2}{\sqrt{2}}$.

For convenience, let us classify the parameter space (e, λ, η) into six regions: We refer regions to the type I if $m_s < m_e$ while to the type II if $m_e < m_\lambda$, as denoted above. According to m_η, each region is further divided into three classes which we denote by a, b and c from large m_η to small m_η, as shown Fig. 4.

Table 1: Mass spectrum around the vacuum $H_1 = H_2 = v/\sqrt{2}$.

fields	NG	gauge	Higgs 1	Higgs 2
mass	0	$m_e = \sqrt{2}\, ev$	$m_\lambda = \sqrt{2}\, \lambda v$	$m_\eta = \sqrt{2}\, \eta v$

Thus the masses of the gauge and Higgs fields remain intact. There exist two Nambu-Goldstone modes for $\eta = 0$. Now, one of the Nambu-Goldstone mode, $\chi = \frac{f_1 - f_2}{\sqrt{2}}$, gets mass $m_\eta = \sqrt{2} v\eta$, while the other mode associated with the spontaneously broken relative $U(1)$ symmetry remains massless.

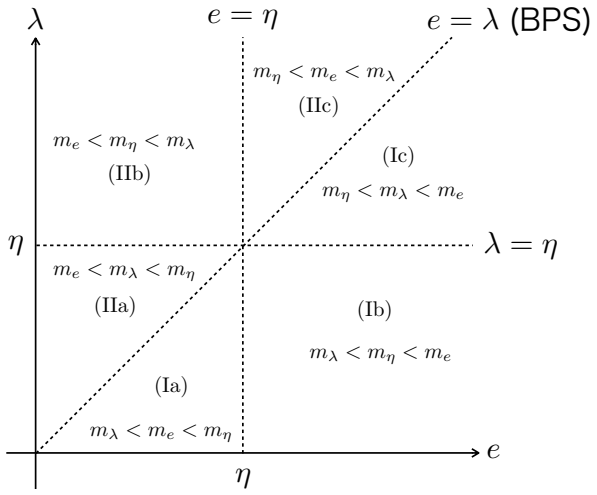

Figure 4: Classification of the parameter space.

The additional potential V_1 in Eq. (3.1) changes the equation of motion for the Higgs fields (2.6) as

$$\mathcal{D}_\mu \mathcal{D}^\mu H_1 = \left[\lambda^2 (v^2 - HH^\dagger) - \eta^2 \left(|H_1|^2 - |H_2|^2\right)\right] H_1, \tag{3.5}$$

$$\mathcal{D}_\mu \mathcal{D}^\mu H_2 = \left[\lambda^2 (v^2 - HH^\dagger) - \eta^2 \left(|H_2|^2 - |H_1|^2\right)\right] H_2. \tag{3.6}$$

The equations of motion for the gauge field are given in Eq. (2.7). The boundary conditions for the Higgs fields at spacial infinity is that in Eq. (3.2). That for the gauge fields will be given below.

3.2 String solutions

3.2.1 General arguments

In what follows, we will concentrate on straight string solutions. For that purpose, we assume the configuration is static, $\partial_0 = 0$, and also we impose $\partial_3 = 0$, namely, the string is parallel

to the x^3 axis.

Let us first concentrate on asymptotic behaviors of the fields. Those for the Higgs fields are given by

$$H_1 \to \frac{v}{\sqrt{2}} e^{ik_1\theta} = \frac{v}{\sqrt{2}} e^{i\frac{k_1+k_2}{2}\theta} e^{i\frac{k_1-k_2}{2}\theta}, \quad H_2 \to \frac{v}{\sqrt{2}} e^{ik_2\theta} = \frac{v}{\sqrt{2}} e^{i\frac{k_1+k_2}{2}\theta} e^{-i\frac{k_1-k_2}{2}\theta}, \tag{3.7}$$

with k_1 and k_2 being arbitrary integers, and $r = \sqrt{x^2+y^2}$ and $\tan\theta = y/x$. Similarly, the asymptotic form of the gauge field is given by

$$A_i \to -\alpha \partial_i \theta = \alpha \epsilon_{ij} \frac{x^j}{r^2}. \tag{3.8}$$

Here, α is the total magnetic flux

$$\alpha = -\frac{1}{2\pi} \int d^2x \; F_{12}. \tag{3.9}$$

Then, the kinetic energy of the Higgs field reads

$$\mathcal{K}_H = \sum_{a=1}^{2} |D_i H_a|^2 \to \left(\frac{v^2}{2} \sum_{a=1}^{2} (k_a - \alpha)^2 \right) r^{-2}. \tag{3.10}$$

Therefore, the tension (mass per unit length) of the string solution is

$$K_H = \int d^2x \; \mathcal{K}_H = 2\pi \left(\frac{v^2}{2} \sum_{a=1}^{2} (k_a - \alpha)^2 \right) \int^{\Lambda} \frac{dr}{r} = \pi v^2 \sum_{a=1}^{2} (k_a - \alpha)^2 \log\Lambda + \cdots, \tag{3.11}$$

where Λ is an IR cutoff (or the size of the system). This is minimized when

$$\alpha = \frac{k_1 + k_2}{2}, \quad K_H = \frac{\pi v^2}{2} (k_1 - k_2)^2 \log\Lambda + \cdots. \tag{3.12}$$

For finite energy configuration (in infinite space $\Lambda \to \infty$), we consider a common integer as $k \equiv k_1 = k_2$. This leads $\alpha = k$, and the string tension becomes finite since the logarithmic divergent term disappears. Namely, we impose the usual finite energy condition

$$D_\mu H_a = \partial_\mu H_a + i A_\mu H_a \to 0, \quad (a = 1, 2) \tag{3.13}$$

at spatial infinity. When we go around the string, both the phases θ_1 and θ_2 of the Higgs fields rotates by $2\pi k_a$ as

$$\frac{1}{2\pi} \oint \vec{\nabla}\theta_a \cdot d\vec{r} = k_a. \tag{3.14}$$

Rephrasing this in terms of $\theta_\pm$, the gauged phase changes by $2\pi k$ while the global phase θ_- is constant as

$$\frac{1}{2\pi}\oint \vec{\nabla}\theta_\pm \cdot d\vec{r} = \frac{1}{2\pi}\oint \vec{\nabla}\frac{\theta_1 \pm \theta_2}{2}\cdot d\vec{r} = \frac{k_1 \pm k_2}{2} \equiv k_\pm. \tag{3.15}$$

We will refer k_+ to the local charge and k_- to the global charge. Namely, this string solution with $(k_1, k_2) = (1, 1)$, or $[k_+, k_-] = [1, 0]$, is purely a local vortex. In the following sections, we will investigate the local string in detail.

Let us describe the generic axially symmetric solution in more details. We make the following ansatz

$$H_a = \frac{v}{\sqrt{2}} e^{ik_a\theta} F_a(r), \quad A_i = \frac{k_1 + k_2}{2}\epsilon_{ij}\frac{x^j}{r^2}A(r). \tag{3.16}$$

The equations of motion for $F_a(r)$ and $A(r)$ read

$$F_1'' + \frac{F_1'}{r} - \left(\frac{k_1 - \frac{k_1+k_2}{2}A}{r}\right)^2 F_1 + \frac{m_\lambda^2}{2}\left(1 - \frac{F_1^2 + F_2^2}{2}\right)F_1 - \frac{m_\eta^2}{4}(F_1^2 - F_2^2)F_1 = 0, \tag{3.17}$$

$$F_2'' + \frac{F_2'}{r} - \left(\frac{k_2 - \frac{k_1+k_2}{2}A}{r}\right)^2 F_2 + \frac{m_\lambda^2}{2}\left(1 - \frac{F_1^2 + F_2^2}{2}\right)F_2 - \frac{m_\eta^2}{4}(F_2^2 - F_1^2)F_2 = 0, \tag{3.18}$$

$$(k_1 + k_2)\left(A'' - \frac{A'}{r}\right) + m_e^2\left[\left(k_1 - \frac{k_1 + k_2}{2}A\right)F_1^2 + \left(k_2 - \frac{k_1 + k_2}{2}A\right)F_2^2\right] = 0. \tag{3.19}$$

3.2.2 Fractional string

Here we consider a global vortex with a fractional flux (local charge) which is not allowed in the $SU(2)$ symmetric model with $\eta = 0$. The simplest example is $(k_1, k_2) = (1, 0)$ for which only H_1 has a nontrivial winding. From Eq. (3.12), we should choose $\alpha = \frac{1}{2}$. The corresponding string tension diverges as

$$K_H\left(\alpha = \frac{1}{2}\right) = \frac{\pi v^2}{2}\log\Lambda + \cdots. \tag{3.20}$$

The logarithmic divergence is universal property for the global strings. Note that the tension of n Abelian global strings is known as $T = 2\pi v^2 n^2 + \cdots$. This formula with Eq. (3.20) implies that out solution with $(k_1, k_2) = (1, 0)$ is the global string with a half winding number $n = \frac{1}{2}$. Similarly, the magnetic flux for this string is $-\pi$ which is a half of that for the integer ANO string as expected from Eq. (3.9). These charges can be understood from the local/global charge of this solution $[k_+, k_-] = \left[\frac{1}{2}, \frac{1}{2}\right]$.

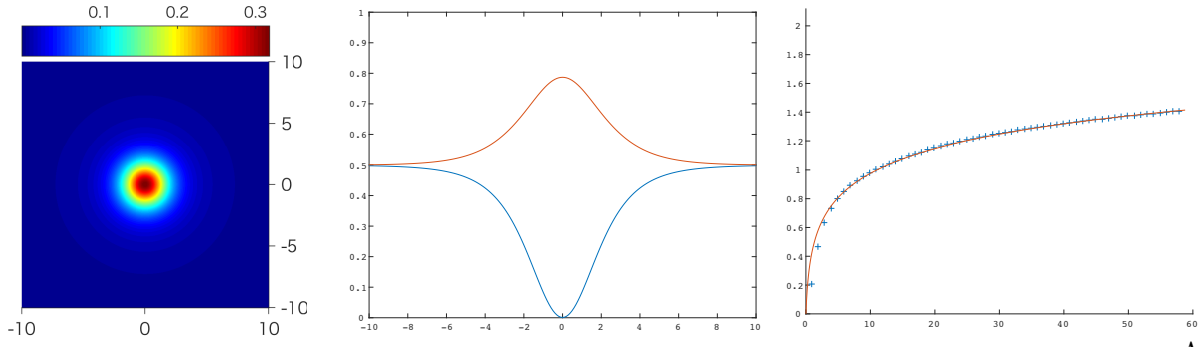

(a) energy density (b) $|H_1|^2$, $|H_2|^2$ (c) tension

Figure 5: $(k_1, k_2) = (1, 0)$ string solution for $(e, \lambda, \eta) = (0.3, 1, 0.25)$. The panel (a) shows the energy density in the xy plane, and (b) shows the profile functions $|H_1|^2$ (blue) and $|H_2|^2$ (red). The tension as a function of the IR cutoff Λ is shown in the panel (c) where the red curve and blue crosses correspond to the analytical expectation curve in Eq. (3.22) and numerical data, respectively.

The minimal string with $(k_1, k_2) = (1, 0)$ is axially symmetric. So we solve Eqs. (3.17) – (3.18) with the following boundary conditions

$$F_1(0) = 0, \quad F_2'(0) = 0, \quad A(0) = 0, \qquad F_1(\infty) = 1, \quad F_2(\infty) = 1, \quad A(\infty) = 1. \tag{3.21}$$

A numerical solution is shown in Fig. 5. The profile function of the winding component H_1 vanishes at the center of the string core, where that of the unwinding component H_2 has non-zero expectation value. The profile functions are shown in the middle panel of Fig. 5. Since this string has a half global string charge, its tension should diverge as explained in Eq. (3.20). We compute the tension $E(\lambda) = 2\pi \int_0^\Lambda dr\, rH$ as a function of the IR cutoff Λ and compare it with analytical expectation formula

$$\frac{E(\Lambda)}{2\pi v^2} = \frac{1}{4} \log \Lambda + \text{const.}\,, \tag{3.22}$$

in the panel (c) of Fig. 5. They agree quite well. We also numerically integrate $F_{12}/2\pi$ and get -0.5000. Thus, our solution indeed have fractional local and global charge $1/2$ and $1/2$.

Next, let us examine asymptotic behavior of the solution by perturbing the fields around the background solution as

$$F_1 = 1 - \frac{f_+(r) + f_-(r)}{2}, \quad F_2 = 1 - \frac{f_+(r) - f_-(r)}{2}, \quad A = 1 - m_e r \tilde{a}(r). \tag{3.23}$$

Then we find

$$f_+'' + \frac{f_+'}{r} - m_\lambda^2 f_+ \;=\; \frac{f_+}{4r^2} - \frac{1}{2r^2} - \frac{3m_\lambda^2}{4} f_+^2 + \frac{m_\lambda^2}{8} f_+^3 + \mathcal{O}(\tilde{a}^2, \tilde{a} f_-, f_-^2), \tag{3.24}$$

$$
\begin{aligned}
f_-'' + \frac{f_-'}{r} - m_\eta^2 f_- &= \frac{f_-}{4r^2} - \frac{m_e\tilde{a}}{r} + \left(\frac{m_e\tilde{a}}{2r} - \left(\frac{m_\lambda^2}{2} + m_\eta^2\right) f_-\right) f_+ \\
&\quad + \frac{1}{4}\left(\frac{m_e\tilde{a}}{2r} - \left(\frac{m_\lambda^2}{2} + m_\eta^2\right) f_-\right) f_+^2 + \mathcal{O}(\tilde{a}^2 f_-, f_-^3), \qquad (3.25) \\
\tilde{a}'' + \frac{\tilde{a}'}{r} - m_e^2\tilde{a} &= \frac{\tilde{a}}{r^2} - \frac{m_e f_-}{r} - \left(m_e^2\tilde{a} - \frac{m_e f_-}{2r}\right) f_+ + \frac{m_e^2}{4}\tilde{a} f_+^2 + \mathcal{O}(\tilde{a} f_-^2). \qquad (3.26)
\end{aligned}
$$

We put two dimensional static propagators at the left hand side, so that the right hand side are the sources due to the string at the origin. The masses of the fluctuations m_+, m_-, m_e for f_+, f_-, a are consistent with those which can be read from Eq. (3.4). To the leading order, f_+ is decoupled with $\tilde{a}$ and f_+. The first equation has an inhomogeneous source $-1/2r^2$ which appears because of the presence of the global string charge. Thus, the fluctuation f_+ decays with inverse power law as

$$
f_+ = q_+ K_{\frac{1}{2}}(m_\lambda r) + \frac{1}{2m_\lambda^2 r^2} + \mathcal{O}\left((m_\lambda r)^{-4}\right), \qquad (3.27)
$$

with $K_{\frac{1}{2}}(mr) = \sqrt{\frac{\pi}{2mr}}\, e^{-mr}$ is the modified Bessel function. The first term is negligible compared with the second term, but we keep it because the subscript $1/2$ of $K_{\frac{1}{2}}(mr)$ is related to a half global string charge. The leading order term $1/2m_\lambda^2 r^2$ is determined by keeping the terms up to the linear order in Eq. (3.24), and we should take $\mathcal{O}(f_+^2, f_+^3)$ into account for obtaining the higher order terms. Note that Eq. (3.24) also includes the terms of order $\mathcal{O}(\tilde{a}^2, \tilde{a} f_-, f_-^2)$ but they are exponentially small and are negligible. The fluctuations f_- and $\tilde{a}$ are exponentially small since their equations of motion does not include inhomogeneous source term. On the other hand, we should not just ignore relatively large factor f_+ in the equations of motion for $\tilde{a}$ and f_+. Generic solution of f_- and $\tilde{a}$ can be written as

$$
f_- = q_- K_{\frac{1}{2}}(m_\eta r) + \delta f_-, \qquad \tilde{a} = q_a K_1(m_e r) + \delta\tilde{a}, \qquad (3.28)
$$

where $K_1(mr) = K_0'(mr)/m$ and $K_0(mr) \sim K_1(mr) \sim K_{\frac{1}{2}}(mr)$ at $mr \gg 1$.

When $m_e > m_\eta$ we ignore terms of order $e^{-m_e r}$. Then we find the next leading order correction as

$$
\begin{aligned}
\delta f_- &= \left(\frac{m_\eta^2\left(2m_\eta^2 + m_\lambda^2\right) - m_e^2\left(2m_\eta^2 + 5m_\lambda^2\right)}{8m_\lambda^2\left(m_e^2 - m_\eta^2\right)}\frac{1}{m_\eta r} + \mathcal{O}(r^{-2})\right) q_- K_{\frac{1}{2}}(m_\eta r), \qquad (3.29) \\
\delta\tilde{a} &= \left(\frac{m_e m_\eta}{m_e^2 - m_\eta^2}\frac{1}{m_\eta r} + \mathcal{O}(r^{-2})\right) q_- K_{\frac{1}{2}}(m_\eta r). \qquad (3.30)
\end{aligned}
$$

When $m_e < m_\eta$, we ignore term of order $e^{-m_\eta r}$ and find

$$
\delta f_- = \left(\frac{m_e^2}{m_\eta^2 - m_e^2}\frac{1}{m_e r} + \mathcal{O}(r^{-2})\right) q_a K_{\frac{1}{2}}(m_e r), \qquad (3.31)
$$

$$\delta\tilde{a} \;=\; \left(\frac{2m_e^4 - m_e^2\left(2m_\eta^2+7m_\lambda^2\right)+3m_\eta^2 m_\lambda^2}{8m_\lambda^2\left(m_\eta^2-m_e^2\right)}\frac{1}{m_e r}+\mathcal{O}(r^{-2})\right) q_a K_{\frac{1}{2}}(m_e r). \tag{3.32}$$

When $m_e = m_\eta$, the leading order in the approximation is $f_- = q_- K_0(m_e r)$ and $\tilde{a} = q_a K_1(m_e r)$. Hence, we conclude that both f_- and $\tilde{a}$ have the same asymptotic behavior $f_- \sim \tilde{a} \sim e^{-mr}$ with $m = \min\{m_e, m_\eta\}$.

3.3 Stabilizing semilocal string by polarization

Next, we consider $k_1 = k_2 = 1$ string. This can be regarded as the pair of $(k_1, k_2) = (1, 0)$ and $(0, 1)$ strings. Although the individual partonic strings have infinite tension due to their global string nature, the $(1, 1)$ string has a finite tension because of the cancelation of the global charges. This implies the existence an attractive force between $(1, 0)$ and $(0, 1)$ strings at large distance. We will see that this is indeed the case if $\eta \neq 0$. Furthermore, we will also find the string solutions can be coaxial or non-coaxial depending on the parameters of the model. For any cases, when we look at the string at sufficiently large distance, the string is almost axially symmetric. Therefore, $F \equiv F_1 \simeq F_2$ asymptotically holds. Assuming this relation, the equations of motion reduce to those for the familiar ANO string

$$F'' + \frac{F'}{r} - \frac{(1-A)^2}{r^2}F + \frac{m_\lambda^2}{2}\left(1-F^2\right)F \simeq 0, \tag{3.33}$$

$$A'' - \frac{A'}{r} + m_e^2\,(1-A)\,F^2 \simeq 0. \tag{3.34}$$

The asymptotic behaviors $F = 1 - f$ and $A = 1 - a$ are well known as

$$f = q_s K_0(m_\lambda r), \quad a = q_a K_1(m_e r). \tag{3.35}$$

The mass parameter m_η does not contribute to determine the asymptotic behaviors in this case, but should affect some local substructure of the semilocal string solutions as we will see below.

The semilocal strings in this model have many interesting features. Among them, the most interesting one is stabilization of the semilocal string in the type II region ($m_e < m_\lambda$) by finite polarization.

Let us start with defining polarization of the semilocal string. As before, let z_1 and z_2 be zeros of H_1 and H_2, respectively. Then the polarization is defined by

$$P = \frac{d}{2}, \quad d \equiv z_1 - z_2, \tag{3.36}$$

where d stands for the displacement vector. We put the factor $1/2$ because the semilocal string can be interpreted as a pair of fractional strings. In order to illustrate the situation,

consider a configuration given by

$$H_1 = v\frac{z-z_1}{\sqrt{|z-z_1|^2+|z-z_2|^2}}, \quad H_2 = v\frac{z-z_2}{\sqrt{|z-z_1|^2+|z-z_2|^2}}. \tag{3.37}$$

Note that these satisfy $|H_1|^2 = |H_2|^2 = v^2/2$. Then, consider a closed contour C_1 encircling only $z = z_1$. When we go around $z = z_1$ along C_1, the phase of H_1 changes by 2π while the phase of H_2 remains intact. This is possible because we have two $U(1)$ symmetries: the one is the gauge symmetry and the other is global symmetry. The $U(1)_{\rm gauge} \times U(1)_{\rm global}$ charges for the configuration like Eq. (3.37) are $(+1, +1)$ for H_1 and $(+1, -1)$ for H_2, respectively. Thus, when we go around $z = z_1$, we travel around $U(1)_{\rm gauge}$ by $+\pi$ and $U(1)_{\rm global}$ by $+\pi$. On the other hand, when we go around $z = z_2$, we travel around $U(1)_{\rm gauge}$ by $+\pi$ and $U(1)_{\rm global}$ by $-\pi$. Namely, H_1 has a half quantized winding number $(\frac{1}{2}, \frac{1}{2})$ while H_2 has a half quantized winding number $(\frac{1}{2}, -\frac{1}{2})$. Thus, a single semilocal string carries the topological charge $+1$ for $U(1)_{\rm gauge}$ and no charges for $U(1)_{\rm global}$, but each fractions$\pm\frac{1}{2}$ fractional winding numbers for $U(1)_{\rm global}$. This is the reason why we put factor $1/2$ in Eq. (3.36). The polarization P is indeed the dipole moment for the $U(1)_{\rm global}$ topological charge.

Note that the polarization for the semilocal string is quite obscure at $\eta = 0$. This is because $U(1)_{\rm global}$ is a subgroup of the manifest $SU(2)$ flavor symmetry. In the $SU(2)$ symmetric model, as is shown in Eq. (2.17), the zeros of Higgs fields can be moved by the $SU(2)$ transformation. Accordingly, the configuration is perfectly axially symmetric, so that the semilocal strings in the model with $\eta = 0$ have no dipole-like behaviors. Nevertheless, as long as we restrict ourselves to the solutions with the fixed boundary condition $|H_1| = |H_2| = v/\sqrt{2}$, the term "polarization", which is usually called "size" in the literature, is still useful. In this sense, we would say the semilocal string at $\eta = 0$ is unpolarized for the type I region, and *infinitely* polarized for the type II region. At the critical point (BPS), the polarization can be freely changed.

Let us now come back to the semilocal string in the type II region for the $\eta \neq 0$ case. The first example is the semilocal string with $(e, \lambda, \eta) = (0.3, 0.6, 0.5)$ which is in the type IIb ($m_e < m_\eta < m_\lambda$). We find the axially symmetric semilocal string, see the panel (a) in Fig. 6. For this solution, we find $|H_1| = |H_2|$ everywhere on the xy plane, so that it is unpolarized. The additional Higgs potential V_1 forces $|H_1|$ and $|H_2|$ to be equal, and therefore the number of flavor is essentially one. Namely, the semilocal string solution is precisely the same as the type II ANO string. Indeed, if we impose $H_1 = H_2$, the terms related to V_1 in the equations of motion vanish and we are left with the equations of motion for the ANO string in the Abelian-Higgs model with one complex scalar. The numerical solution shown in the panel (a) in Fig. 6 is obtained by the energy relaxation process explained in Appendix A. If we further

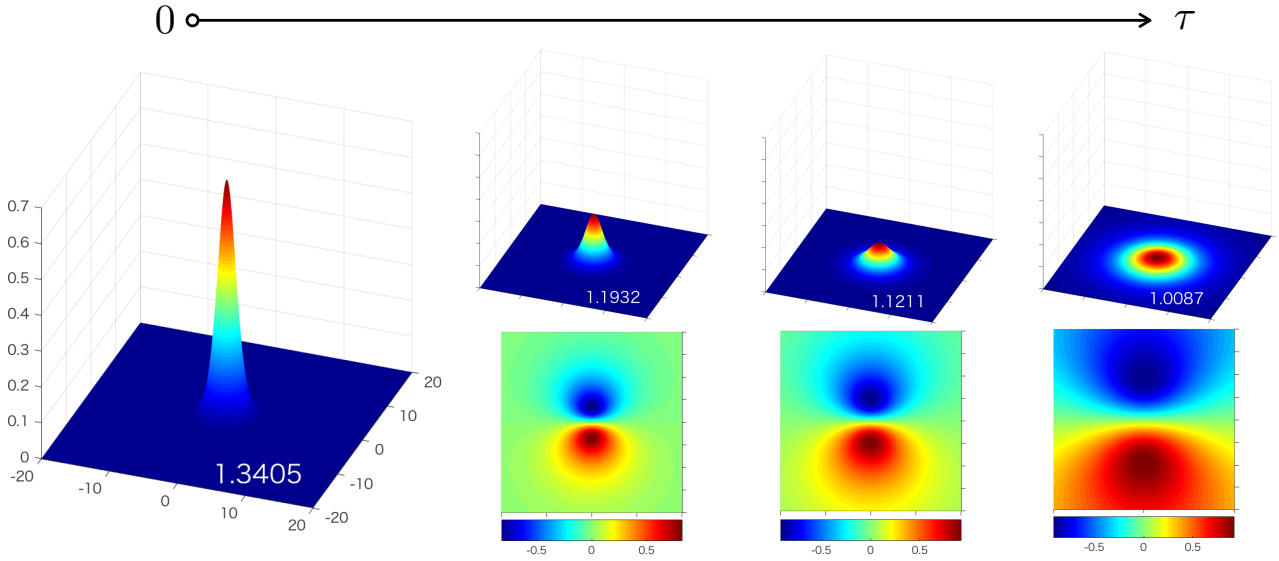

Figure 6: (a) Energy density plot of the stable semilocal string in the type IIb with $(e, \lambda, \eta) = (0.3, 0.6, 0.5)$ and $v = 1$. The string is axially symmetric and is unpolarized because $|H_1| = |H_2|$ everywhere. (b) Snapshots of the 2nd energy relaxation evolution for $\eta = 0$ with taking the configuration in the panel (a) as an initial configuration at $\tau = 0$. The upper panels show the energy densities (the axes are the same as those of (a)) and the lower panels show $H\tau_3 H^\dagger$. The numerical values plotted in the upper panels are the tension in the unit of $2\pi v^2$.

try to sweep out energy by continuing the imaginary time evolution, we find that changes are pretty tiny, which proves the solution already reaches the convergent point. Now, let us see what will happen as τ goes by after we suddenly turn off $\eta \to 0$. Namely, we perform the 2nd relaxation process with the configuration shown in Fig. 6(a) for $\eta = 0$. The model with $\eta = 0$ is in the type II region $(e, \lambda, \eta) = (0.3, 0.6, 0)$ of the $SU(2)$ symmetric model. Therefore, the initial configuration is no longer stable and dilutes to the vacuum, see also the effective potential given in Fig. 2. In the panels in Fig. 6(b), we show several snapshots for the transition. The semilocal vortex expands with axially symmetric shape being kept. The plots in the bottom line of Fig. 6(b) shows $H\tau_3 H^\dagger$ for each moment. The darkest red point corresponds to zero of H_1 while the darkest blue point to zero of H_2 ($H\tau_3 H^\dagger$ is initially zero everywhere). It is clearly seen that the dilution of the type II semilocal string in the $SU(2)$ symmetric model is accompanied by $|z_1 - z_2| \to \infty$ as expected. Thus, the role of the additional potential V_1 is to prevent $d = z_1 - z_2$ from flying to infinity. Indeed, the additional Higgs potential energetically prefer $H_1 = H_2$ to $H_1 \neq H_2$. This is reason why the semilocal string does not expand for $\eta \neq 0$.

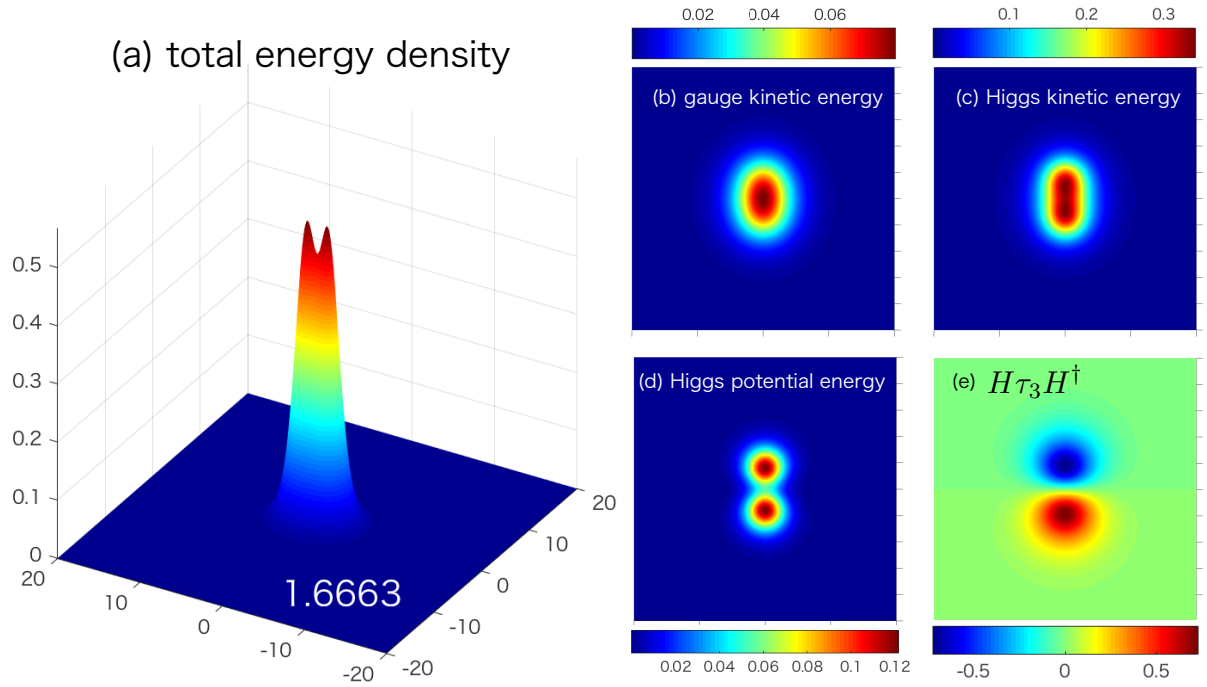

Figure 7: Energy densities of the single semilocal string with two partons. The parameters are $v = 1$ and $(e, \lambda, \eta) = (0.3, 1.2, 0.5)$. The panels (a) – (e) show the total energy density, the gauge kinetic energy $F_{12}^2/2e^2$, the Higgs kinetic energy $\sum_a |\mathcal{D}_i H_a|^2$, the Higgs potential energy $V_0 + V_1$, and $H\tau_3 H^\dagger$, respectively. The total energy density peaks are located at $(\pm 1.2/v, 0)$ and the Higgs zeros are at $(\pm 1.7/v, 0)$. The plot regions for the four small panels are $[-10, 10]^2$. The number at the corner in (a) is the tension in the unit of $2\pi v^2$.

For the above parameter choice $(e, \lambda, \eta) = (0.3, 0.6, 0.5)$, the effect of V_1 is relatively too strong. As a consequence, z_1 is stuck to z_2 and the semilocal string is unpolarized. This solution is less interesting because it is precisely same as the type II ANO string in the Abelian-Higgs model with a single Higgs field. One may expect that if we weaken the effect of V_1, the displacement $d = z_1 - z_2$ is neither infinity nor zero. It is indeed the case. As a typical example, let us take $(e, \lambda, \eta) = (0.3, 1.2, 0.5)$. The value $\lambda = 1.2$ is twice bigger than the previous one. The corresponding semilocal string solution is shown in Fig. 7. As is clearly shown, the configuration is not axially symmetric, and the total energy density shown in Fig. 7(a) has two peaks at $(x, y) = (\pm 1.2/v, 0)$. The total energy density is the sum of the gauge kinetic contribution in Fig. 7(b), the Higgs kinetic contribution in Fig. 7(c), and the Higgs potential energy in Fig. 7(d). The gauge kinetic energy is elliptic shape with a single peak at the origin, whereas the Higgs potential has sharp two peaks whose locations are almost coincide with the Higgs zeros $(x, y) = (\pm 1.7/v, 0)$ which are identical to the positions

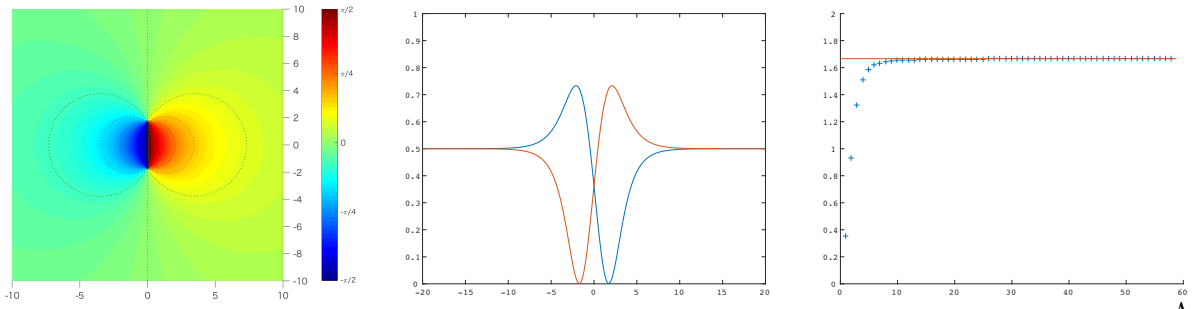

(a) θ_{12} (b) $|H_1|^2$, $|H_2|^2$ (c) tension

Figure 8: (a) The relative phase θ_{12} in the xy plane for the semilocal string with $(e, \lambda, \eta) = (0.3, 1.2, 0.5)$. (b) The profile funtions of H_1 (red) and H_2 (blue). (c) The tension in the unit of $2\pi v^2$ as a function of IR cutoff Λ. The red line shows the asymptotic value 1.6663 and the blue crosses are numerically obtained value of $T(\Lambda)$.

of positive and negative peaks of $H\tau_3 H^\dagger$ shown in Fig. 7(e). In order to see the expected dipole structure in this solution, it is worth to plot the relative phase

$$\theta_{12} = \frac{1}{2}\arg(H_1/H_2) \tag{3.38}$$

as shown in Fig. 8. There is a branch cut between $(x, y) = (-1.7/v, 0)$ and $(1.7/v, 0)$. When we go around the lower/upper branch point, θ_{12} changes by $+\pi/-\pi$. Namely, the semilocal string is a dipole of the half quantized global $U(1)$ charges. The polarization is given by

$$P = \frac{1.7}{2v}. \tag{3.39}$$

We also show the amplitudes of the Higgs fields in Fig. 8(b), in which one can clearly see H_1 and H_2 have zeros at different points. Finally, in order to check if the tension is finite, we plot $T(\Lambda) = \int_0^\Lambda dr \int_0^{2\pi} d\theta\, r\mathcal{H}$ in Fig. 8(c). As shown in the figure, $T(\Lambda)$ rapidly converges to a finite value. This is sharp contrast to $[\frac{1}{2}, \frac{1}{2}]$ string solution shown in Fig. 5, where $T(\lambda)$ is logarithmically divergent. The string solution here has $[1, 0] = [\frac{1}{2}, \frac{1}{2}] + [\frac{1}{2}, -\frac{1}{2}]$ has zero net global charge, so that the tension remains finite as usual local strings.

3.4 Phase diagram

In this subsection, we will survey the parameter space (e, λ, η). Especially, we are interested in clarifying when the semilocal vortex is polarized. Before doing this, let us remind that the usual ANO string in the Abelian-Higgs model with one complex scalar field is essentially controlled by one dimensionless parameter

$$\gamma = \frac{m_e}{m_\lambda}. \tag{3.40}$$

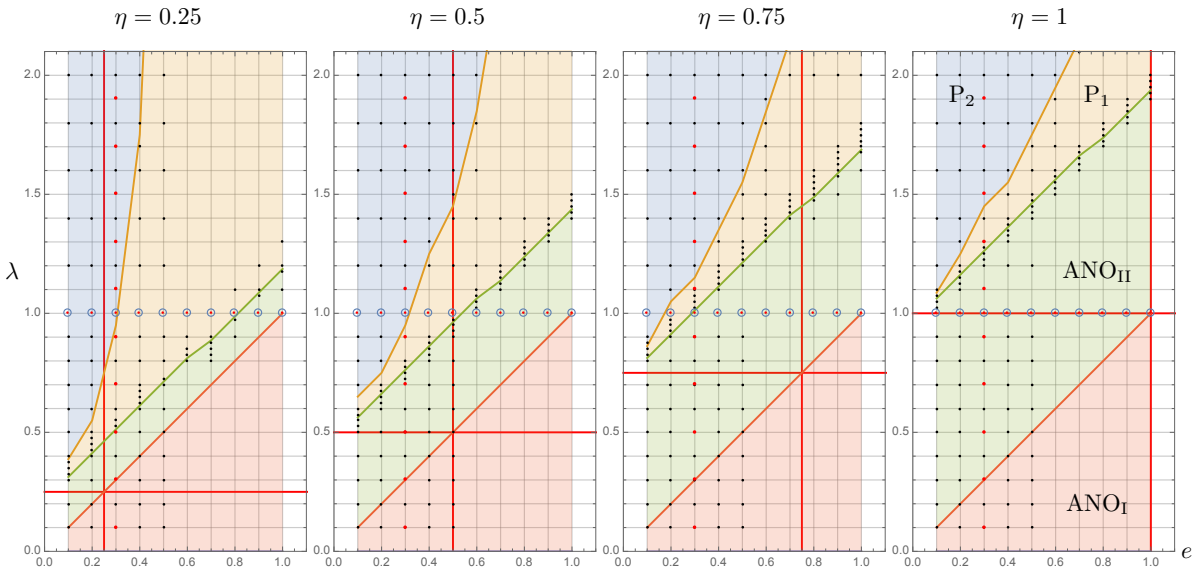

Figure 9: Phases of the $(k_1, k_2) = (1, 1)$ string in the e-λ plane with fixed values of $\eta = 0.25, 0.5, 0.75, 1$. The four regions, $\mathrm{ANO_I}$, $\mathrm{ANO_{II}}$, P_1 and P_2, correspond to pink, green, yellow and blue regions, respectively. $\mathrm{ANO_C}$ corresponds to the points on the line $e = \lambda$. The parameters for which we obtained numerical solutions are expressed by the markers on cites. The red and orange lines correspond to the dashed lines in Fig. 4 dividing the parameter space into six regions.

The ANO string solutions with different (m_e, m_λ) and (m'_e, m'_λ) are essentially the same solution up to overall coordinate rescaling if $m_e/m_\lambda = m'_e/m'_\lambda$ holds. This is the reason why the ANO strings are classified into three types: the type I ($\gamma > 1$), type II ($\gamma < 1$) and the critical (BPS) ($\gamma = 1$). In our model, we have four different masses 0, m_e, m_λ and m_η. Therefore, classification of the strings in our model is more complicated. For example, even in the case of $m_e/m_\lambda = m'_e/m'_\lambda$, the corresponding string solutions might essentially be different.

We classify the solutions into 2 categories: The ANO type or polarized (P) (or molecular) type according to the displacement $d = 0$ or $d \neq 0$, respectively. (We refer the ANO string by an unpolarized string.) Looking into the details, the ANO type can further be classified into $\mathrm{ANO_I}$, $\mathrm{ANO_{II}}$ and $\mathrm{ANO_C}$ according to $m_\lambda < m_e$, $m_e < m_\lambda$, and $m_e = m_\lambda$. Similarly, the P type is decomposed into $\mathrm{P_1}$ ($\mathrm{P_2}$) for configuration with one peak (two peaks) in the total energy density. For example, the configuration given in Fig. 6(a) is of the type $\mathrm{ANO_{II}}$, and the solution in Fig. 7 is of the type $\mathrm{P_2}$. In Fig. 9, we show the e-λ plane with fixed values of $\eta = 0.25, 0.5, 0.75, 1$. The parameters for which we really obtained numerical solutions are expressed by the markers on cites in Fig. 9. Observing the phase diagram in Fig. 9, we soon

realize that there are stable strings in the type II region ($e < \lambda$) where the usual semilocal string at $\eta = 0$ is unstable. Indeed, we find finite energy and finite size string solutions for all $|\eta| > 0$. Namely, the type II semilocal strings are stabilized as long as η is nonzero, in contrast to the common knowledge that type-II semilocal strings should be unstable.

Let us see how the string configuration changes as varying the parameters.

For concreteness, first, we change λ with e and η being fixed, namely move vertically in Fig. 9. Let us focus on the strings with $e = 0.3$ which correspond to the red-dotted cites in each panels of Fig. 9. The corresponding energy densities for the red cites are shown in Fig. 10. The strings with $\lambda < e$ in the left-most column are of the $\mathrm{ANO_I}$ type and those in the second column from left are of the BPS type. Increasing λ beyond the BPS line ($e = \lambda$), the strings now enter the $\mathrm{ANO_{II}}$ region. All these strings are unpolarized because the Higgs fields are forced to be $H_1 = H_2$ at any spacetime points. Departing further from BPS line toward larger λ, now the configurations transit to be polarized. Namely, H_1 and H_2 have zeros at different points. The string cross section is elongated, so that shape of the total energy density becomes elliptic with single peak ($\mathrm{P_1}$) for relatively small λ as can be seen for example $\lambda = 0.7$, 0.9 in the top line of Fig. 10, or acquires two peaks ($\mathrm{P_2}$) for sufficiently large λ as can be seen in the panels with $\lambda \geq 1.1$ in the top line of Fig. 10. The relation between the displacement $|d|$ and λ for $e = 0.3$ and $\eta = 0.25$ is shown in Fig. 12. Universal feature for changing λ under fixing e is that d is zero below a certain $\lambda_0(\eta)$, and $|d|$ increases above $\lambda_0(\eta)$. It seems that $|d|$ converges to an upper value $|d_{\max}(\eta)|$ for $\lambda \to \infty$, see Fig. 12(a). The critical value $\lambda_0(\eta)$ as a function of η is a monotonically increasing function. We also find that $|d_{\max}(\eta)|$ is a monotonically decreasing function of η.

Next, we fix λ and η, and vary e. It is horizontal movement in the e-λ plane in Fig. 9. As typical configurations, we look at the strings with $\lambda = 1$ which correspond to the red-dotted cites inside blue circle in Fig. 9. The corresponding total energy density are shown in Fig. 11. The displacement $|d|$ tends to be larger for smaller e while it becomes zero for e above a certain critical $e_0(\eta)$. The detailed relation between $|d|$ and e is shown in Fig. 12(a). As opposed to large λ limit, $|d|$ becomes steeply large at e vanishing limit. The critical value $e_0(\eta)$ as a function of η is a monotonically decreasing function.

Finally, let us see what happens when we vary η with e and λ being fixed. As can be seen in Figs. 10 and 11, the displacement $|d|$ becomes small when we increase η. However, once the string becomes unpolarized, the configuration is frozen. Namely, it is not further deformed even if we further increase η.

From above observations, we find an inclination for $|d|$ to become larger when we come deeper into the type II region ($e \ll \lambda$). This behavior may be expected if we recall the well-

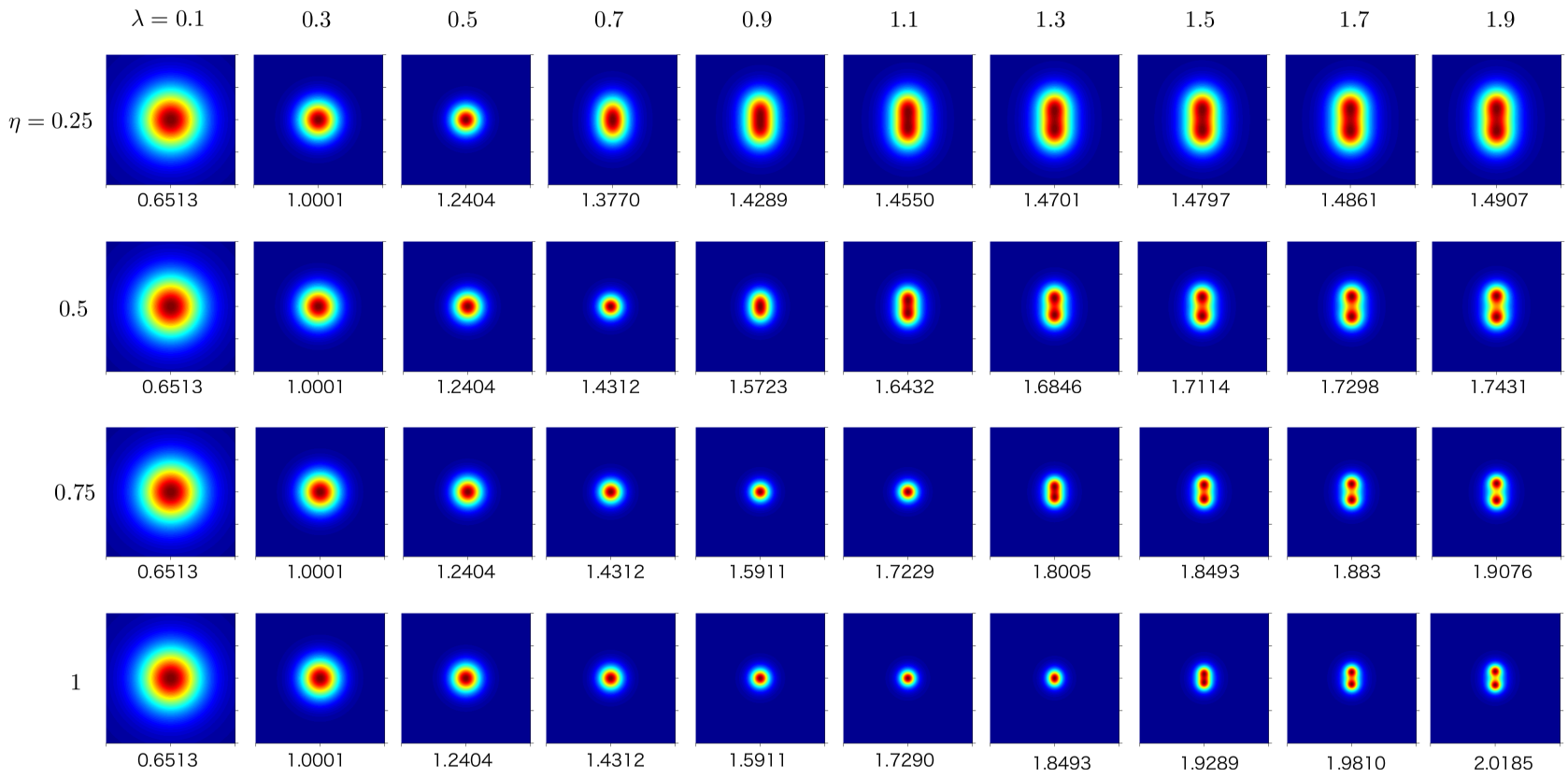

Figure 10: Numerical solutions for λ-η plane with $e = 0.3$. The numerical values below the figures are the tension in the unit of $2\pi v^2$.

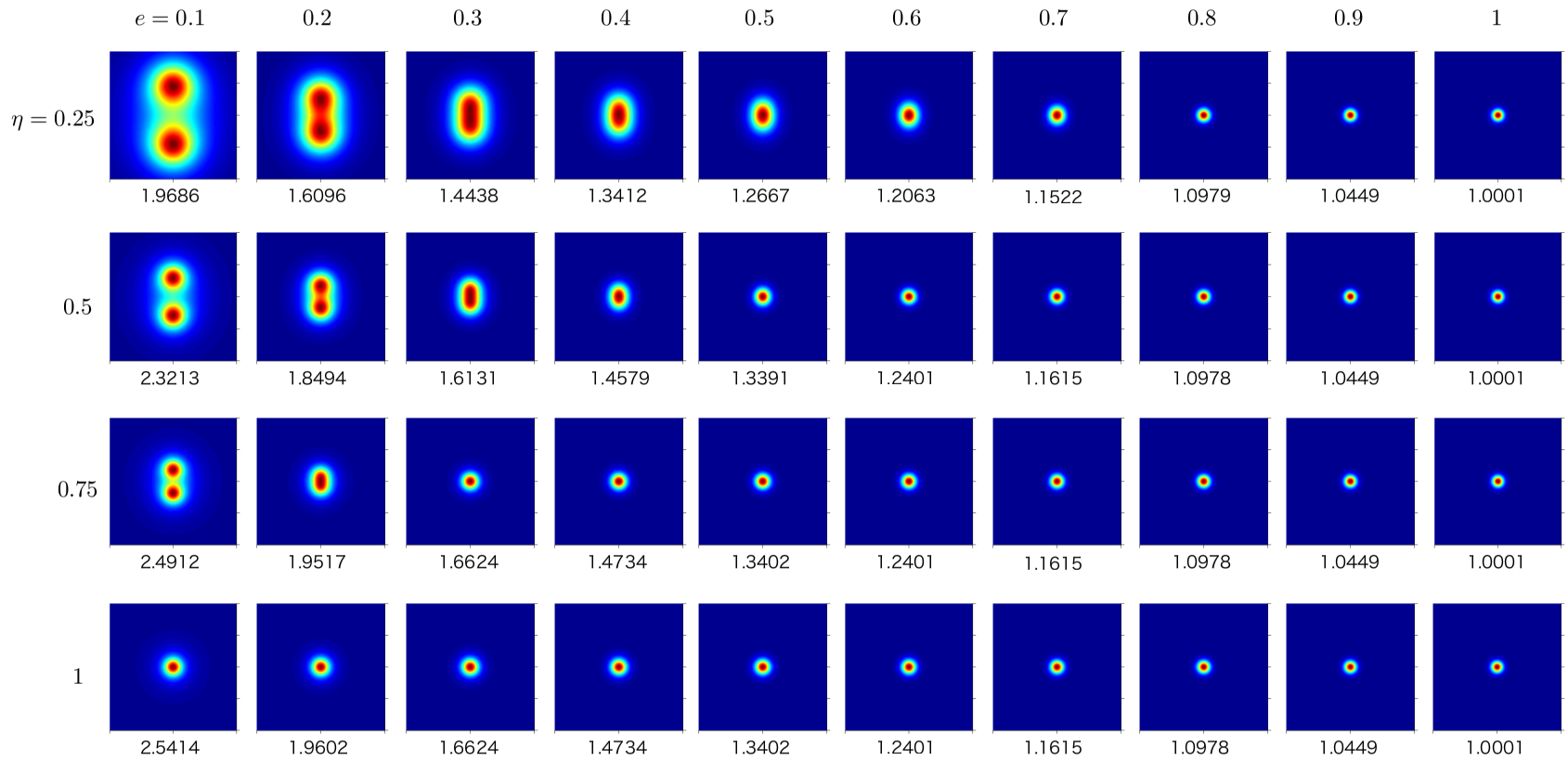

Figure 11: Numerical solutions for e-η plane with $\lambda = 1$. The numerical values below the figures are the tension in the unit of $2\pi v^2$.

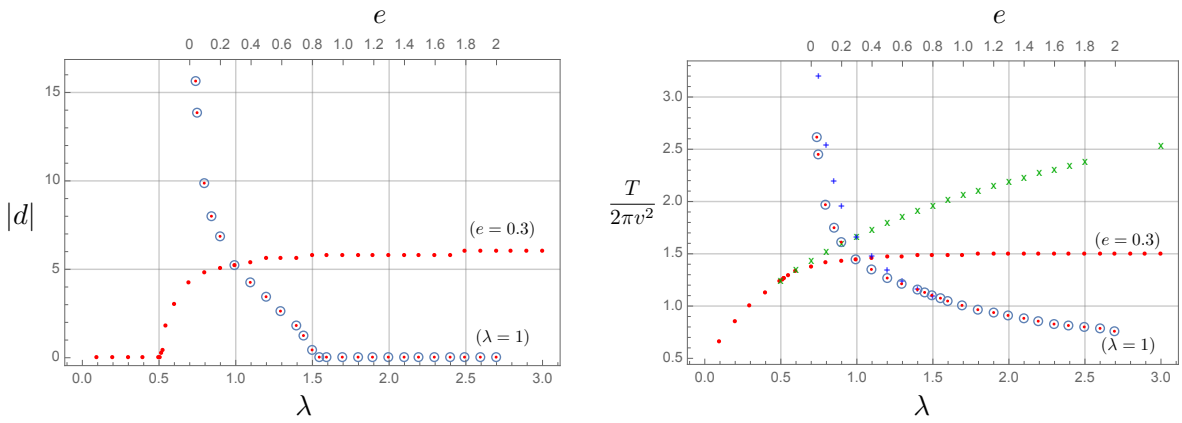

Figure 12: Displacement (a) and tension (b) as functions of e and λ for $\eta = 0.25$. The corresponding solutions (the red-dotted cites and the red-dotted cites in the blue circle) are shown in the left-most panel of Fig. 9 and the subfigures in the top columns of Figs. 10 and 11. In the panel (b), the green crosses (blue crosses) show the tension as a function of λ (e) for the ANO solutions in the $\eta = 0$ limit.

known fact that two integer ANO strings repel in the type II region as is already mentioned. However, our strings are not integer ANO strings but two strings with fractional local and global charges. Indeed, we find that both two limits $e \to 0$ and $\lambda \to \infty$ with η being fixed lead to the polarization, but they are qualitatively different. The displacement d diverges at the former limit while it converges to a finite value in the latter limit. From numerical observation in Fig. 9, we have an estimation for the critical values $\lambda_0(\eta)$ and $e_0(\eta)$ as functions of η as

$$\lambda_0(\eta) - e_0(\eta) \simeq \eta. \tag{3.41}$$

This equation explains the existence of the unpolarized $\mathrm{ANO_{II}}$ string in the band $e < \lambda \lesssim e+\eta$ (the light-green region in Fig. 9). The polarized $\mathrm{P}_{1,2}$ string appears in the region $\lambda \gtrsim e + \eta$ which is above the $\mathrm{ANO_{II}}$-band (the light-blue and light-orange regions in Fig. 9). Note that the $\mathrm{ANO_{II}}$-band closes when $\eta = 0$, and the polarized strings become unstable because their polarizations become infinite. In terms of the classification by (IIa/IIb/IIc) as given in Fig. 4, we find that the only $\mathrm{ANO_{II}}$ string appears in the IIa region. Both the $\mathrm{ANO_{II}}$ and $P_{1,2}$ are possible in the IIb and IIc regions, but the dominant part of the IIb region is occupied by P_2 strings while the IIc region is dominated by P_1 strings.

4 Summary and discussion

The semilocal strings exist in the extended Abelian-Higgs model with the two complex scalars with the $SU(2)$ symmetry. It has been known that the semilocal strings are stable only in the type I parameter region $m_e > m_\lambda$ but unstable to expand in the type-II parameter region $m_e < m_\lambda$. In this paper, we have studied stabilization of the semilocal strings by the polarization in the presence of the additional $SU(2)$ breaking potential given in Eq. (3.1). We have found that the semilocal strings in the type II region ($m_e < m_\lambda$) become stable against expansion by the additional potential. The single semilocal string splits into two fractional strings with opposite global charges $\pm 1/2$. Thus, the semilocal string is polarized. It is crucial that the non-Abelian flavor symmetry is broken by the additional potential, which allows the existence of fractionally charged string with 1/2 local and 1/2 global charge. We have obtained the numerical solutions for the fractional strings for various parameters. We also have investigated the asymptotic behaviors and have found that they decay exponentially with the smallest masses of the fields at the bulk, which are quite different from those of the well-known ANO strings and usual semilocal strings. We further have studied dependence of the polarization of the single semilocal string on the masses m_e, m_λ and m_η in detail. We have found that the semilocal string is stable in the whole parameter region. Especially, the type II region $m_e < m_\lambda$ is divided into two phases. In one of them, the unpolarized semilocal strings, namely the type-II ANO solutions, appear for $m_e < m_\lambda < m_e + m_\eta$. In the other region $m_\lambda > m_e + m_\eta$, the two Higgs fields have zeros at different points, namely the strings are polarized. The displacement $|d|$ of the two zeros is larger for smaller m_e. It also increases as m_λ is increased, but it saturates some upper value.

Before closing this paper, several discussions are addressed here.

We have studied only a single vortex in this paper. Multiple vortices including the interaction among them are an important next step. In particular, two neighboring vortices will enhance their polarizations because of attraction between fractional vortices belonging to each other. For a small number of vortices, vortex molecules may constitute a vortex polygon, that is vortices sit at the vertices of a polygon, as the case of two-component BECs [30]. For a large number of vortices, we may expect that they constitute a vortex lattice when the system size is finite, as the case of conventional type-II superconductors in the presence of an applied magnetic field. In the $SU(2)$ symmetric extended Abelian Higgs model of $\eta = 0$, a vortex lattice will be difficult to be realized from the following reason. Vortices are unstable in the type-II region and stable in the type-I region. However, in the type-I region, vortices are attractive and so superconductors are unstable against the applied magnetic field. As shown in

this paper, in the presence of the additional potential term ($\eta \neq 0$), semilocal vortices become stable even in the type-II region. Consequently, these superconductors are stable against the applied magnetic field, in which a vortex lattice will be formed. The form of vortex lattice may be similar to that of two-component BECs under the rotation [22, 23, 25, 26, 28, 29] or that of two-gap superconductors where vortices are polarized [21].

If we consider a potential term

$$V_2 = \frac{\eta^2}{2}(H\tau_3 H^\dagger - r^2)^2 = \frac{\eta^2}{2}(|H_1|^2 - |H_2|^2 - r^2)^2, \tag{4.1}$$

instead of Eq. (4.1) considered in this paper, the fluxes of fractional vortices deviate from 1/2. This phenomenon is known for multi-gap superconductors, multi-component BECs, and $\mathbb{C}P^1$ lumps.

In addition to the potential term in Eq. (4.1) that we considered in this paper, we may further add the potential term $\mathrm{Tr}(H\tau_2 H^\dagger)$. This is known as an intrinsic Josephson interaction term. In this case, two fractional vortices constituting a single semilocal vortex will be connected by a sine-Gordon kink, as the case of two-gap superconductors [48, 19] or coherently coupled two-component BECs [24, 29].

In this paper, we have studied the extended Abelian-Higgs model with two Higgs fields. Generalization to N Higgs fields is possible, where semilocal vortices reduce to $\mathbb{C}P^{N-1}$ sigma model lumps in the strong gauge coupling limit. In this case, we may add a potential term

$$V_2 = \sum_a \frac{\eta_a^2}{2}\mathrm{Tr}(Hh_a H^\dagger)^2 \tag{4.2}$$

where h_a are all possible Cartan generators of $SU(N)$. Then, one semilocal vortex is split into N fractional vortices with $1/N$ quantized fluxes. Further adding Josephson terms $\mathrm{Tr}(HE_{ij}H^\dagger)$ with E_{ij} having a nonzero (i,j) component is also interesting, by which i-th and j-th fractional vortices are connected. The total configuration would form a vortex graph, as the case of multi-component BECs [31, 33].

Acknowledgments

This work is supported by the Ministry of Education, Culture, Sports, Science (MEXT)-Supported Program for the Strategic Research Foundation at Private Universities "Topological Science" (Grant No. S1511006), and the Japan Society for the Promotion of Science (JSPS) Grant-in-Aid for Scientific Research (KAKENHI Grant No. 25400268). The work of M. E. is supported in part by JSPS Grant-in-Aid for Scientific Research (KAKENHI Grant

No. 26800119). The work of M. N. is supported in part by a Grant-in-Aid for Scientific Research on Innovative Areas "Topological Materials Science" (KAKENHI Grant No. 15H05855) and "Nuclear Matter in Neutron Stars Investigated by Experiments and Astronomical Observations" (KAKENHI Grant No. 15H00841) from the MEXT of Japan.

A Numerical recipe

We numerically solve the equations of motion (2.7), (3.5) and (3.6) under a static assumption as $A_{1,2}(x^1, x^2)$ and $H(x^1, x^2)$. We make an ansatz $A_0 = A_3 = 0$, and take a gauge $\partial_1 A_1 + \partial_2 A_2 = 0$ throughout this paper. Instead of solving directly the equations of motion for the fileds $X = \{A_1, A_2, H_a\}$, we will solve the following gradient flow equations

$$\partial_i^2 X(x^1, x^2, \tau) + \mathcal{U}(X(x^1, x^2, \tau)) = \partial_\tau X(x^1, x^2, \tau), \tag{A.1}$$

where an ideal time τ-dependence is introduced. The original equations of motion are obtained by letting the right hand side to be zero. With an appropriate initial function $X_0 = X(x^1, x^2, \tau = 0)$ which has qualitatively the same behaviors as Eq. (3.7), we solve the time evolution of $X(x^1, x^2, \tau)$. Typically, $\partial_\tau X$ gradually goes to zero as the time evolution. As a consequence, we get the solution $X(x^1, x^2, \tau = \infty)$ to the original equation of motion. Our computational box is typically $[-60, 60]^2$ divided into 1200^2 lattice points, and we will solve the gradient flow equation (A.1) by the Crank-Nicolson type method. We take the Neumann boundary conditions for all the fields.

In the following, we will set $v = 1$. In other words, we will use rescaled variables as

$$\tilde{x}^\mu = v x^\mu, \quad \tilde{A}_\mu = A_\mu / v, \quad \tilde{H} = H/v. \tag{A.2}$$

Then, v dependence disappears from Eqs. (2.7) and (3.5). We will not distinguish X and $\tilde{X}$ unless stated otherwise.

References

[1] A. A. Abrikosov, "On the Magnetic properties of superconductors of the second group," Sov. Phys. JETP **5**, 1174 (1957) [Zh. Eksp. Teor. Fiz. **32**, 1442 (1957)].

[2] H. B. Nielsen and P. Olesen, "Vortex Line Models for Dual Strings," Nucl. Phys. B **61**, 45 (1973). doi:10.1016/0550-3213(73)90350-7

[3] T. Vachaspati and A. Achucarro, "Semilocal cosmic strings," Phys. Rev. D **44**, 3067 (1991). doi:10.1103/PhysRevD.44.3067

[4] A. Achucarro and T. Vachaspati, "Semilocal and electroweak strings," Phys. Rept. **327**, 347 (2000) [Phys. Rept. **327**, 427 (2000)] doi:10.1016/S0370-1573(99)00103-9 [hep-ph/9904229].

[5] J. Urrestilla, N. Bevis, M. Hindmarsh, M. Kunz and A. R. Liddle, "Cosmic microwave anisotropies from BPS semilocal strings," JCAP **0807**, 010 (2008) doi:10.1088/1475-7516/2008/07/010 [arXiv:0711.1842 [astro-ph]].

[6] M. Hindmarsh, "Existence and stability of semilocal strings," Phys. Rev. Lett. **68**, 1263 (1992). doi:10.1103/PhysRevLett.68.1263

[7] A. Achucarro, K. Kuijken, L. Perivolaropoulos and T. Vachaspati, "Dynamical simulations of semilocal strings," Nucl. Phys. B **388**, 435 (1992). doi:10.1016/0550-3213(92)90621-H

[8] M. Shifman and A. Yung, "Non-Abelian semilocal strings in N=2 supersymmetric QCD," Phys. Rev. D **73**, 125012 (2006) doi:10.1103/PhysRevD.73.125012 [hep-th/0603134].

[9] M. Eto, J. Evslin, K. Konishi, G. Marmorini, M. Nitta, K. Ohashi, W. Vinci and N. Yokoi, "On the moduli space of semilocal strings and lumps," Phys. Rev. D **76**, 105002 (2007) doi:10.1103/PhysRevD.76.105002 [arXiv:0704.2218 [hep-th]].

[10] M. Eto, K. Hashimoto, G. Marmorini, M. Nitta, K. Ohashi and W. Vinci, "Universal Reconnection of Non-Abelian Cosmic Strings," Phys. Rev. Lett. **98**, 091602 (2007) doi:10.1103/PhysRevLett.98.091602 [hep-th/0609214].

[11] G. W. Gibbons, M. E. Ortiz, F. Ruiz Ruiz and T. M. Samols, "Semilocal strings and monopoles," Nucl. Phys. B **385**, 127 (1992) doi:10.1016/0550-3213(92)90097-U [hep-th/9203023].

[12] M. Hindmarsh, "Semilocal topological defects," Nucl. Phys. B **392**, 461 (1993) doi:10.1016/0550-3213(93)90681-E [hep-ph/9206229].

[13] M. Hindmarsh, R. Holman, T. W. Kephart and T. Vachaspati, "Generalized semilocal theories and higher Hopf maps," Nucl. Phys. B **404**, 794 (1993) doi:10.1016/0550-3213(93)90597-I [hep-th/9209088].

[14] M. Eto and M. Nitta, "Semilocal Fractional Instantons," JHEP **1603**, 067 (2016) doi:10.1007/JHEP03(2016)067 [arXiv:1512.07458 [hep-th]].

[15] E. Babaev, "Vortices carrying an arbitrary fraction of magnetic flux quantum in two gap superconductors," Phys. Rev. Lett. **89**, 067001 (2002) doi:10.1103/PhysRevLett.89.067001 [cond-mat/0111192].

[16] E. Babaev, A. Sudbo and N. W. Ashcroft, "A Superconductor to superfluid phase transition in liquid metallic hydrogen," Nature **431**, 666 (2004) doi:10.1038/nature02910 [cond-mat/0410408]; E. Babaev and N. W. Ashcroft, "Violation of the London law and Onsager-Feynman quantization inmulticomponent superconductors," Nature Phys. **3**, 530 (2007).

[17] J. Smiseth, E. Smorgrav, E. Babaev and A. Sudbo, "Field and temperature induced topological phase transitions in the three-dimensional N-component London superconductor," Phys. Rev. B **71**, 214509 (2005) doi:10.1103/PhysRevB.71.214509 [cond-mat/0411761].

[18] A. Gurevich and V. M. Vinokur, Phys. Rev. Lett. **90**, 047004 (2003).

[19] J. Goryo, S. Soma and H. Matsukawa, "Deconfinement of vortices with continuously variable fractions of the unit flux quanta in two-gap superconductors," Euro Phys. Lett. **80**, 17002 (2007). [arXiv:cond-mat/0608015].

[20] M. Nitta, M. Eto, T. Fujimori and K. Ohashi, "Baryonic Bound State of Vortices in Multicomponent Superconductors," J. Phys. Soc. Jap. **81**, 084711 (2012) doi:10.1143/JPSJ.81.084711 [arXiv:1011.2552 [cond-mat.supr-con]].

[21] A. Crisan, Y. Tanaka, D. D. Shivagan, A. Iyo, L. Cosereanu, K. Tokiwa, and T. Watanabe, "Anomalous AC Susceptibility Response of (Cu,C)Ba2Ca2Cu3Oy: Experimental Indication of Two-Component Vortex Matter in Multi-Layered Cuprate Superconductors," Jpn. J. Appl. Phys. **46**, L451-L453 (2007); Y. Tanaka, A. Crisan, D. D. Shivagan, A. Iyo, K. Tokiwa, and T. Watanabe, Jpn. J. Appl. Phys. **46**, 134-145 (2007); A. Crisan, A. Iyo, Y. Tanaka, H. Matsuhata, D. D. Shivagan, P. M. Shirage, K. Tokiwa, T. Watanabe, T. W. Button, and J. S. Abell, "Magnetically coupled pancake vortex molecules in HgBa2Can-1CunOy ($n \geq 6$)," Phys. Rev. **B** 77, 144518 (2008); J. W. Guikema, H. Bluhm, D. A. Bonn, R. Liang, W. N. Hardy, and K. A. Moler, "Two-dimensional vortex behavior in highly underdoped YBa2Cu3O6+x observed by scanning Hall probe microscopy," Phys. Rev. **B** 77, 104515 (2008); L. Luan, O. M. Auslaender, D. A. Bonn, R. Liang, W. N. Hardy, and K. A. Moler, "Magnetic force microscopy study of interlayer

kinks in individual vortices in the underdoped cuprate superconductor YBa2Cu3O6+x" Phys. Rev. **B** 79, 214530 (2009).

[22] E. J. Mueller and T.-L. Ho, "Two-Component Bose-Einstein Condensates with a Large Number of Vortices," Phys. Rev. Lett. **88**, 180403 (2002).

[23] K. Kasamatsu, M. Tsubota and M. Ueda, "Vortex Phase Diagram in Rotating Two-Component Bose-Einstein Condensates," Phys. Rev. Lett. **91**, 150406 (2003).

[24] D. T. Son, M. A. Stephanov, "Domain walls in two-component Bose-Einstein condensates," Phys. Rev. A**65**, 063621 (2002).

[25] K. Kasamatsu, M. Tsubota and M. Ueda, "Vortex Molecules in Coherently Coupled Two-Component Bose-Einstein Condensates," Phys. Rev. Lett **93**, 250406 (2004).

[26] K. Kasamatsu, M. Tsubota and M. Ueda, "Vortices in multicomponent Bose-Einstein condensates," Int. J. Mod. Phys. **B** 19, 1835 (2005).

[27] M. Eto, K. Kasamatsu, M. Nitta, H. Takeuchi and M. Tsubota, "Interaction of half-quantized vortices in two-component Bose-Einstein condensates," Phys. Rev. A **83**, 063603 (2011) doi:10.1103/PhysRevA.83.063603 [arXiv:1103.6144 [cond-mat.quant-gas]].

[28] A. Aftalion, P. Mason and W. Juncheng, "Vortex-peak interaction and lattice shape in rotating two-component Bose-Einstein condensates," Phys. Rev. A **85**, 033614 (2012).

[29] M. Cipriani and M. Nitta, "Crossover between integer and fractional vortex lattices in coherently coupled two-component Bose-Einstein condensates," Phys. Rev. Lett. **111**, 170401 (2013) doi:10.1103/PhysRevLett.111.170401 [arXiv:1303.2592 [cond-mat.quant-gas]].

[30] M. Kobayashi and M. Nitta, "Vortex polygons and their stabilities in Bose-Einstein condensates and field theory," J. Low. Temp. Phys. **175**, 208 (2014) doi:10.1007/s10909-013-0977-4 [arXiv:1307.1345 [cond-mat.quant-gas]].

[31] M. Eto and M. Nitta, "Vortex trimer in three-component Bose-Einstein condensates," Phys. Rev. A **85**, 053645 (2012) doi:10.1103/PhysRevA.85.053645 [arXiv:1201.0343 [cond-mat.quant-gas]].

[32] M. Cipriani and M. Nitta, "Vortex lattices in three-component Bose-Einstein condensates under rotation: simulating colorful vortex lattices in a color superconductor," Phys. Rev. A **88**, 013634 (2013) doi:10.1103/PhysRevA.88.013634 [arXiv:1304.4375 [cond-mat.quant-gas]].

[33] M. Eto and M. Nitta, "Vortex graphs as N-omers and CP(N-1) Skyrmions in N-component Bose-Einstein condensates," Europhys. Lett. **103**, 60006 (2013) doi:10.1209/0295-5075/103/60006 [arXiv:1303.6048 [cond-mat.quant-gas]].

[34] M. Nitta, M. Eto and M. Cipriani, "Vortex molecules in Bose-Einstein condensates," J. Low. Temp. Phys. **175**, 177 (2013) doi:10.1007/s10909-013-0925-3 [arXiv:1307.4312 [cond-mat.quant-gas]].

[35] B. J. Schroers, "Bogomolny solitons in a gauged O(3) sigma model," Phys. Lett. B **356**, 291 (1995) doi:10.1016/0370-2693(95)00833-7 [hep-th/9506004].

[36] B. J. Schroers, "The Spectrum of Bogomol'nyi solitons in gauged linear sigma models," Nucl. Phys. B **475**, 440 (1996) doi:10.1016/0550-3213(96)00348-3 [hep-th/9603101].

[37] M. Nitta and W. Vinci, "Decomposing Instantons in Two Dimensions," J. Phys. A **45**, 175401 (2012) doi:10.1088/1751-8113/45/17/175401 [arXiv:1108.5742 [hep-th]].

[38] A. Alonso-Izquierdo, W. G. Fuertes and J. Mateos Guilarte, "Two species of vortices in massive gauged non-linear sigma models," JHEP **1502**, 139 (2015) doi:10.1007/JHEP02(2015)139 [arXiv:1409.8419 [hep-th]]; A. Alonso-Izquierdo and J. Mateos-Guilarte, "Higgs phase in a gauge $\mathbf{U}(1)$ non-linear $\mathbf{CP}^1$-model. Two species of BPS vortices and their zero modes," arXiv:1607.00188 [hep-th].

[39] J. Jaykka and M. Speight, "Easy plane baby skyrmions," Phys. Rev. D **82**, 125030 (2010) doi:10.1103/PhysRevD.82.125030 [arXiv:1010.2217 [hep-th]].

[40] M. Kobayashi and M. Nitta, "Fractional vortex molecules and vortex polygons in a baby Skyrme model," Phys. Rev. D **87**, no. 12, 125013 (2013) doi:10.1103/PhysRevD.87.125013 [arXiv:1307.0242 [hep-th]].

[41] S. B. Gudnason and M. Nitta, "Fractional Skyrmions and their molecules," Phys. Rev. D **91**, no. 8, 085040 (2015) doi:10.1103/PhysRevD.91.085040 [arXiv:1502.06596 [hep-th]].

[42] M. Eto and M. Nitta, "Color Magnetic Flux Tubes in Dense QCD," Phys. Rev. D **80**, 125007 (2009) doi:10.1103/PhysRevD.80.125007 [arXiv:0907.1278 [hep-ph]].

[43] M. Eto, Y. Hirono, M. Nitta and S. Yasui, "Vortices and Other Topological Solitons in Dense Quark Matter," PTEP **2014**, no. 1, 012D01 (2014) doi:10.1093/ptep/ptt095 [arXiv:1308.1535 [hep-ph]].

[44] A. P. Balachandran, S. Digal and T. Matsuura, "Semi-superfluid strings in high density QCD," Phys. Rev. D **73** (2006) 074009 doi:10.1103/PhysRevD.73.074009 [hep-ph/0509276].

[45] E. Nakano, M. Nitta and T. Matsuura, "Non-Abelian strings in high density QCD: Zero modes and interactions," Phys. Rev. D **78**, 045002 (2008) doi:10.1103/PhysRevD.78.045002 [arXiv:0708.4096 [hep-ph]]. M. Eto, E. Nakano and M. Nitta, "Effective world-sheet theory of color magnetic flux tubes in dense QCD," Phys. Rev. D **80**, 125011 (2009) doi:10.1103/PhysRevD.80.125011 [arXiv:0908.4470 [hep-ph]]. M. Eto, M. Nitta and N. Yamamoto, "Instabilities of Non-Abelian Vortices in Dense QCD," Phys. Rev. Lett. **104**, 161601 (2010) doi:10.1103/PhysRevLett.104.161601 [arXiv:0912.1352 [hep-ph]].

[46] M. Eto, Y. Isozumi, M. Nitta, K. Ohashi and N. Sakai, "Moduli space of non-Abelian vortices," Phys. Rev. Lett. **96**, 161601 (2006) doi:10.1103/PhysRevLett.96.161601 [hep-th/0511088].

[47] M. Eto, Y. Isozumi, M. Nitta, K. Ohashi and N. Sakai, "Solitons in the Higgs phase: The Moduli matrix approach," J. Phys. A **39**, R315 (2006) doi:10.1088/0305-4470/39/26/R01 [hep-th/0602170].

[48] Y. Tanaka, "Phase instability in multi-band superconductors, " J. Phys. Soc. Jp. **70**, 2844 (2001); "Soliton in Two-Band Superconductor," Phys. Rev. Lett. **88**, 017002 (2001).